HHS Public Access

Author manuscript

Dev Biol. Author manuscript; available in PMC 2016 October 15.

Published in final edited form as:

Dev Biol. 2015 October 15; 406(2): 203–211. doi:10.1016/j.ydbio.2015.08.019.

nlz1 is required for cilia formation in zebrafish embryogenesis

Sunit Dutta[1], **Shahila Sriskanda**[1], **Elangovan Boobalan**[1], **Ramakrishna. P. Alur**[1], **Abdel Elkahloun**[2], and **Brian P. Brooks**[1]

[1]Unit on Pediatric, Developmental & Genetic Ophthalmology, Ophthalmic Genetics and Visual Function Branch, National Eye Institute, National Institutes of Health, Bethesda, MD 20892, USA

[2]Microarray Core, National Human Genome Research Institute, National Institutes of Health, Bethesda, MD 20892, USA

Abstract

The formation of cilia is a fundamental developmental process affecting diverse functions such as cellular signaling, tissue morphogenesis and body patterning. However, the mechanisms of ciliogenesis during vertebrate development are not fully understood. In this report we describe a novel role of the Nlz1 protein in ciliogenesis. We demonstrate morpholino-mediated knockdown of *nlz1* in zebrafish causes abnormal specification of the cells of Kupffer's vesicle (KV); a severe reduction of the number of cilia in KV, the pronephros, and the neural floorplate; and a spectrum of later phenotypes reminiscent of human ciliopathies. *In vitro* and *in vivo* data indicate that Nlz1 acts downstream of Foxj1a and Wnt8a/presumed canonical Wnt signaling. Furthermore, Nlz1 contributes to motile cilia formation by positively regulating Wnt11/presumed non-canonical Wnt signaling. Together, our data suggest a novel role of *nlz1* in ciliogenesis and the morphogenesis of multiple tissues.

Keywords

Kupffer's vesicle; motile cilia; Wnt; Nlz1; Foxj1; Left-right asymmetry

Introduction

Cilia are microscopic, hair-like organelles on the surface of almost all vertebrate cell types (Zaghloul and Brugmann, 2011). Cilia are comprised of an ordered array of microtubule elements and are generally divided into two categories based on structural and functional differences, namely, motile and non-motile (primary) cilia (Garcia-Gonzalo and Reiter, 2012).. Motile cilia are generally longer than non-motile cilia; and, as their name implies, they beat in a directional fashion to promote fluid flow along the epithelial cell surfaces of the lung, brain, and kidney. In contrast, non-motile or primary cilia are short and are present in nearly all cell types in vertebrates. They are often specialized for sensory functions (e.g.,

Correspondence to: Brian P. Brooks.

olfaction, osmoregulation, thermosensation, vision (Dorn et al., 2012; Lancaster et al., 2011; McEwen et al., 2008). Several recent studies demonstrate that multiple cellular signaling pathways (e.g., Hedgehog (Hh), Wnt, planar cell polarity (PCP), platelet-derived growth factor (PDGF), NOTCH and fibroblast growth factors (FGF)) play pivotal roles in ciliogenesis; in turn, cilia can form a "hub" around which cellular signaling can occur (Ajima and Hamada, 2011; Corbit et al., 2005; Ferrante et al., 2009; Neugebauer et al., 2009; Norris and Grimes, 2012; Przemeck et al., 2003). Impaired formation or functioning of cilia is associated with a wide spectrum of human diseases, collectively termed ciliopathies (Fliegauf et al., 2007; Hildebrandt et al., 2011)

The external body pattern of vertebrates is bilaterally symmetric, in contrast to the conserved left-right (LR) asymmetric pattern of internal organs like the heart, stomach, and liver. Congenital abnormalities in this patterning in humans are termed heterotaxies (*situs ambiguous*). Establishment of the LR axis happens during early embryo development, much ahead of morphological organ asymmetry. Initially the left and right sides are determined purely in reference to anterior –posterior and dorsal-ventral axes of the embryo. During gastrulation, bilateral symmetry is broken by complex cellular/developmental mechanisms that generate directional fluid flow, resulting in asymmetric expression of genes, like *lefty* in the lateral plate mesoderm (LPM) (Hamada et al., 2002). This directional fluid flow first appears in the node (in mouse)/Kupffer's vesicle (KV, in zebrafish), propelled by the beating of motile cilia. Mouse and zebrafish mutants with no cilia, absence of ciliary motility, and defects in cilia length/number demonstrate abnormal fluid flow in the node/KV and disruption of LR asymmetry (Kramer-Zucker et al., 2005; Neugebauer et al., 2009; Nonaka et al., 1998; Supp et al., 1997). All these observations support a strong correlation between motile cilia and initiation of LR asymmetry. However, the precise mechanism by which motile cilia-derived fluid flow in the node/KV establishes LR asymmetry is still unknown (Babu and Roy, 2013).

Genetic analysis in mouse, *Xenopus*, and zebrafish identified a critical role of a forkhead transcription factor, *FoxJ1*/*foxj1a* in motile cilia formation (Gomperts et al., 2004; Huang et al., 2003; Stubbs et al., 2008; Yu et al., 2008). Recently, Caron et al. demonstrated that canonical Wnt signaling regulates *foxj1a* and motile cilia formation (Caron et al., 2012). However, the relationship between cilia formation and Wnt signaling is complex and not fully understood (Wallingford and Mitchell, 2011). For example, ciliogenesis itself may, in turn, inhibit canonical Wnt signaling and non-canonical Wnt/PCP effector molecules may affect (and be affected by) ciliogenesis (Ferrante et al., 2009; Kishimoto et al., 2008). The precise mechanism by which canonical Wnt and non-canonical Wnt/PCP signaling regulate ciliogenesis is still not completely understood.

In this report we describe a novel role of the zinc-finger containing protein, Nlz1/nlz1 (zfp703, znf703, Zeppo1, noz1), in motile cilia formation in zebrafish. Previously, our lab demonstrated that *nlz1* is required for proper closure of the ventral optic fissure during eye development; inhibition of nlz1 activity resulted in uveal coloboma (Brown et al., 2009). Here, we extend these studies to show that Nlz1 is essential for motile cilia formation in the zebrafish embryo downstream of the ciliary "master transcription factor", *foxj1a*. We demonstrate that knockdown of *nlz1* in zebrafish results in depletion of cilia during

embryogenesis, producing a phenotype reminiscent of a human ciliopathy. Nlz1 expression in zebrafish is positively regulated by canonical Wnt-β catenin signaling, whereas overexpression of the Nlz1 protein inhibits Wnt-β catenin signaling in cultured cells. Nlz1 also acts as a positive regulator of Wnt11/presumed non-canonical Wnt signaling in the process of motile cilia formation. Together, our results suggest a critical role of *nlz1* in motile cilia formation and function in vertebrates.

Materials and Methods

Animal maintenance and embryos

Wild-type AB and ABXTL zebrafish lines were raised and maintained at 28°C according to standard protocol (Westerfield, 2000). Embryos were obtained from natural spawning and staged according to Kimmel (Kimmel et al., 1995).

Plasmids and constructs

The open reading frames (ORF) of zebrafish *nlz1*, zebrafish *foxj1a*, human *NLZ1*, and human *FOXJ1* were subcloned into pCS2^{+}. The zebrafish *nlz1mutant* construct has a nonsense mutation, c.C996G, introducing a TAG stop codon at p.Y332 (p.Y332X).

Whole-mount *in situ* hybridization and Alcian blue staining

In situ hybridization was performed according to standard protocol (Thisse and Thisse, 2008); two color *in situ* hybridization was performed using anti-digoxygenin, and anti-fluorescein antibodies (Roche) (Hauptmann and Gerster, 1994). The following digoxygenin or fluorescein probes were used: *nlz1*, *sox32*, *podocin*, *wt1a*, *pck1a*, *cdh17*, and *charon.* 5d old embryos were fixed in 4% PFA and Alcian blue staining of craniofacial elements was done as described in (Barrallo-Gimeno et al., 2004). A Leica M205 FA dissecting scope was used to observe live and *in situ* stained embryos.

Morpholino, RNA and Dextran injection

Nlz1 MO1 (5′ATCCAGGAGGCAGTTCGCTCATCTG 3′) and Nlz1 MO2 (5′CGGGTGTTCAGTT TTCATTTAGAGA3′, used for confirmation of the phenotype), Wnt8.1a (Lewis et al., 2004) and Foxj1a (5′CATGGAACTCATGGAGAGCATGGTC 3′), and standard control MO (5′ATCCAGGAGGCAGTTCGCTCATCTG3′) were obtained from Gene Tools. We predominantly use Nlz1 MO1 in this paper unless otherwise stated. Zebrafish embryos were injected at the 1–2 cell stage at the following concentrations: 1–3.5ng Nlz1 MO1, 5ng of Nlz1 MO2, 5ng Foxj1a MO, and 2ng Wnt8.1a MO. To target dorsal forerunner cells (DFC), 3′-fluorescein tagged MOs and mRNA were injected into the yolk at the ~512 cell stage (DFC^{MO}, DFC^{RNA}) (Amack and Yost, 2004). mRNA was synthesized using the mMESSAGE mMACHINE kit (Ambion). 20–100 pg of capped mRNA was injected into 1 cell stage embryos. Larvae were anesthetized and rhodamine conjugated dextran 70,000 (Molecular Probes) was injected into the hindbrain ventricle. DIC images were captured by a Leica DFC 420C digital camera. Injection experiments were repeated three times.

Western Blot and Quantitative real-time RT-PCR (qRT-PCR)

Zebrafish embryos at 30h stage were de-yolked and lysed as described by Westerfield (Westerfield, 2000). Samples were loaded into TGX Precast gels (Biorad) and transferred to PVDF membrane. Immunoblotting was done using anti-Nlz1 (1:500 dilution) and anti-β-tubulin (1:1000 dilution) primary antibody and detected with IRDye800CW and IRDye 680RD secondary antibody (1:25,000 dilution, LI-COR). Blots were scanned with ODESSY CLX infrared imaging system (LI-COR). Total RNA from zebrafish embryos was isolated at 1S stage and qRT-PCR was performed as described in (Lan et al., 2009).

LiCl treatment

Dechorionated zebrafish embryos were incubated in embryo medium containing either 0.2 M LiCl (from 50% epiboly to 70% epiboly) or 0.1 M LiCl (from 50% epiboly to 20h). The embryos were washed several times with embryo medium and incubated to the desired stage. Cultured cells were treated with 0.03M LiCl for 10 h prior to harvest for the Topflash luciferase assay.

Topflash luciferase assay

HEK293T cells were cultured in the media proposed by ATCC, supplemented with 10% fetal bovine serum. Cells were transfected with X-treme GENE HP (Roche) transfection reagent and fixed or harvested 48–72h after transfection. Human *NLZ1 (HNLZ1)* and *β-Catenin* plasmid constructs were used for transfection. Luciferase assays were performed using a dual-luciferase reporter assay system (Promega) following manufacturer's guidelines. HEK293T cells were plated in a 24 well plate and transfected at 80% confluence with 0.8μg plasmid DNA/well, including Renila luciferase (0.020 μg/well), Topflash-luciferase (0.20 μg/well), and other plasmid DNA as indicated.

Imaging

Confocal microscopy was done using a Leica Sp2 (Leica, Switzerland).

Results

Knockdown of *nlz1* in zebrafish embryos results in defects reminiscent of a human ciliopathy

We previously observed that zebrafish embryos injected with either translation blocking- or splice site blocking-Nlz1 MO at the 1 cell stage develop uveal coloboma, a potentially blinding congenital ocular malformation in humans (Brown et al., 2009; Chang et al., 2006). Examination of the *nlz1* morphant embryos at different developmental stages, however, revealed a plethora of defects in several organ systems. At 48 hours post-fertilization (h) the *nlz1* morphant fish (3.5ng Nlz1MO1 injected) showed a short anterior-posterior (A–P) axis, a curved tail, and heart edema (Fig. 1A–B). A similar phenotype was observed when a different, non-overlapping translational blocking MO (5ng Nlz1 MO2 injected) against *nlz1* was used (data not shown). Because these findings could be non-specific and/or off-target, we performed several important controls. 1) The Nlz1 MO mediated knockdown resulted in reduced levels of Nlz1protein in morphants (Fig. 1Q). 2) The morphant phenotype was not

rescued by co-injection of Nlz1 MO1 and P53 MO, suggesting nonspecific apoptosis was not primarily responsible (Fig. S1B). 3) Severe (class II and class III) morphant phenotypes (Fig. S1A–B) resulting from injection of Nlz1 MO1, Nlz1 MO2, and co-injection of MO1 and MO2 at different doses, were partially rescued by co-injection of *nlz1* mRNA (Fig. S1C). 4) A mutant version of *nlz1* (Mut *nlz1*) mRNA, in contrast, did not rescue the *nlz1* morphant phenotype (Fig. S1D). 5) Lastly, we have used the CRISPR/Cas9 system to target the *nlz1* locus. Germline transmission of the Cas9-induced mutations in the target site was observed in the F1 progeny of interbred F0 founders (Fig. S2E). The CRISPR-Cas9 F1 mutants ($nlz1^{-/-}$) exhibited a curved tail, heart edema, and ocular coloboma, similar to *nlz1* morphants (Fig. S2A, B). Taken together, these observations suggest that the morpholino phenotype is a *bone fide* result of a decrease in *nlz1* expression. As such, unless otherwise noted, the morphant phenotypes are described.

Further phenotypic characterization of the *nlz1* morphants demonstrated that injection of rhodamine dextran into the hindbrain ventricles at 28h resulted in abnormal fluid flow into the forebrain, consistent with a congenital brain malformation and/or hydrocephalus (Fig. 1A–B, inset). Morphants also exhibited cystic kidneys (Fig. 1C–D); small otic vesicles with three--rather than twootoliths (Fig. 1E–F); uveal coloboma (Fig. 1G–H); a smaller KV at the 5 somite (S) stage (Fig. 1I, J); facial dysmorphology as demonstrated by staining of cartilage at 120h (Fig. 1K,L); and loss of *podocin* (a glomerular marker) expression (Fig. 1M,N). Interestingly, *cdh17* (a pronephric duct marker) and *wt1* (a transcription factor expressed in the cells of pronephric field) expression (Fig. 1O,P, data not shown) were unaltered in the developing kidneys. Abnormal otolith numbers, and brain defects were also observed in the *nlz1* knockout embryos (Figure S2B). Taken together, these anatomic findings were suggestive of defective cilia function in morphant/mutant fish (Hildebrandt et al., 2011).

Left-right asymmetry defects in Nlz1 MO-injected embryos

Given that cilia in KV are necessary to establish direction fluid flow and, therefore, left-right asymmetry in zebrafish (Essner et al., 2005), we assayed the expression pattern of two Nodal pathway genes [*southpaw (spw)*, and *lefty2 (lft2)*] that are normally expressed on the left side of the lateral plate mesoderm. Whereas control embryos showed the expected left-sided asymmetry (Fig. 2A, D), both *nlz1* morphants injected at the 1–2 cell stage, and $DFC^{nlz1\ MO}$ showed bilateral (Fig. 2B, E), right-sided (Fig. 2B′, E′) or complete loss of expression for the two markers (data not shown), in addition the laterality defects observed in the morphant fish was dose dependent (Fig. S3). Similarly, the left-sided heart tube jogging marked by cardiac myosin light chain 2 (*cmlc2*) expression in control embryos was reversed to either right-sided or in the midline in morphants (Fig. 2H,H′). Co-injection of *HNLZ1* mRNA with Nlz1 MO in 1–2 cell stage, and $DFC^{Nlz1\ MO+HNLZ1\ RNA}$ was able to partially rescue these laterality defects (Fig. 2C, F, I). Similarly, the normal heart looping marked by *cmlc2* expression observed in wild-type ($nlz^{+/+}$) embryos was randomized in *nlz1* knockout embryos (Fig. S2C). Thus *nlz1* plays a critical role in left-right asymmetry in zebrafish.

nlz1 is expressed in KV cells and is necessary for KV specification and cilia formation

To better understand the relationship between *nlz*1 and ciliated structures such as KV, we next examined the expression pattern of *nlz1* during development and assessed the effect of MO knockdown of *nlz1* expression on ciliogenesis. Whole mount *in-situ* hybridization at the 1S stage revealed that DFCs-the *sox32*-positive cells that migrate and organize to form KV (Oteiza et al., 2008) co-expressed *nlz1* and *sox32* (Fig. 3A, B). At 50% epiboly stage, *nlz1* expression was first visualized in the marginal cells (Fig. S4C, C′); at 90% epiboly, *nlz1* expression was restricted to the posterior region and in DFCs (Fig. S4D, D′). Later in development, *nlz1* is expressed in the tail-bud, the mid-hindbrain boundary, the pronephros, and in trunk somites (Fig. S4E, E′, F, F′).

Given that Nlz1 morphants exhibited a hypoplastic KV on DIC imaging (Fig. 1J), we next assayed expression of a pan-KV marker *cha* (*dand5*) after Nlz1 MO injection in 1 cell stage or DFC$^{nlz1\ MO}$ injection. Both approaches led to severe down-regulation of *cha* expression at the 1S stage, whereas *sox32* expression in DFCs remained unaltered (Fig. 3C, D). These results suggest that Nlz1 is important for KV cell, but not DFC, specification.

Next we assessed cilia formation in *nlz1* morphants and control embryos at different developmental stages. In *nlz1*morphants (injection in 1cell stage or DFC$^{Nlz1\ MO}$ injection), motile cilia formation was inhibited in KV, the neural floor plate and the pronephros, compared to control MO-injected embryos (Fig. 3E, F, H–K). Similarly, motile cilia formation was inhibited in the KV of CRISPR-Cas9 F1 mutant embryos (Fig. S2D). The effect of Nlz1 MO-mediated inhibition of KV cilia formation can be partially rescued by co-injection of *nlz1* mRNA (human and zebrafish orthologs) in 1 cell stage and in DFC$^{Nlz1\ MO+\ nlz1RNA}$ (Fig. 3G,L) embryos. However, overexpression of *nlz1* was unable to induce ectopic or increased cilia formation (data not shown).

foxj1a acts upstream of *nlz1* during ciliogenesis

Recent studies in zebrafish and *Xenopus* found that the transcription factor Foxj1a plays a “master regulatory” role in cilia formation; *foxj1a* morphants exhibit defects in cilia formation and KV specification similar to *nlz1* morphants (Stubbs et al., 2008; Yu et al., 2008). To understand the epistatic relationship between *foxj1a* and *nlz1*, we injected Foxj1a MO and assayed *nlz1* expression at 1S stage. *foxj1a* morphants exhibit severe down-regulation of *nlz1* expression in the posterior dorsal region, and in KV (Fig. 4A′, B′); however, *nlz1* expression in the anterior brain region remain unaltered in *foxj1a* morphants (Fig. 4A,B). In contrast, Nlz1MO-injected fish did not show any visible change in the *foxj1a* expression pattern compared to controls (Fig. S5). Similar to the previous reports, KV cilia formation was down-regulated in *foxj1a* morphants at 5S stage (Fig. 4E), and *foxj1a* morphants also showed left-right asymmetric defects assayed by expression of *lft2* and *cmlc2* (Fig. 4G, H). The loss of the KV cilia phenotype was partially rescued by overexpressing *nlz1* mRNA in *foxj1a* morphants, at the 1 cell stage or in DFC$^{Nlz1\ MO+foxj1a\ RNA}$ (Fig. 4F, Fig. 3L); similarly, the laterality defects of *foxj1a* morphants was partially rescued by overexpressing *nlz1* RNA in *foxJ1a* morphants (Fig. 4G,H). These observations led us to hypothesize that Nlz1 functionally acts downstream of Foxj1a.

To specifically address this hypothesis, we analyzed the human *NLZ1* promoter region *in silico* and found a sequence (TGTGTTGC, at position −905 to −912 upstream of the *NLZ1* transcription start site) that is similar to the FOXJ1 consensus binding sites TGTNNTGT (Lim et al., 1997) and TGTGGTGC (Lin et al., 2004). Expression of FOXJ1 in HEK293T cells co-transfected with a reporter construct containing ~2kb of *NLZ1* promoter sequence upstream of the luciferase gene led to a 4–5 fold increase in reporter expression compared to empty vector control (Fig. S6A). To ascertain if FOXJ1 acted as a direct upstream regulator of *NLZ1*, we performed a chromatin immunoprecipitation (ChIP) assay in ARPE-19 cells transiently transfected with a *FOXJ1* expression construct. ChIP from transfected cells followed by PCR using primers flanking the consensus element showed FOXJ1 can bind to the consensus sequence in the *NLZ1* upstream region (Fig. S6B), similarly, injection of *foxj1a* m-RNA at 1 cell stage induces ectopic expression of *nlz1* (Fig. S7B,B′) thus supporting a direct role of *FOXJ1* in regulating *NLZ1*expression.

Wnt/β-catenin signaling regulates Nlz1

The canonical Wnt signaling pathway plays a major role in animal development by influencing processes such as cell division and cell fate specification (Grigoryan et al., 2008). Recent evidence supports a role of canonical Wnt signaling in ciliogenesis, at least in part, through a *foxj1a*-dependent mechanism (Caron et al., 2012). To test whether canonical Wnt signaling regulates *nlz1* expression, we injected a MO against *wnt8a* (classically, a canonical Wnt ligand) (Hsieh et al., 1999) and demonstrated that *nlz1* expression was down-regulated or absent in morphants at 1S (Fig. 4A,A′,C,C′). Similarly, activation of Wnt/β-catenin signaling by LiCl treatment resulted in expansion of *nlz1* expression (Fig. 4I–L). To our surprise, activation of Wnt/β-catenin signaling by LiCl in *foxj1a* morphants rescues *nlz1* expression in the KV (Fig. 4D′), suggesting a Foxj1a- independent activation of Nlz1 via canonical Wnt signaling. Conversely, TOP-Flash luciferase assays in HEK-293T cells demonstrate that activation of Wnt/β-catenin signaling either by LiCl or by β-catenin was repressed by NLZ1(Fig. 4M), consistent with a biochemical feedback mechanism.

Wnt11 is functionally downstream of Nlz1

Non-canonical Wnt signaling has been implicated in ciliogenesis and cilia, in turn, have been shown in some systems to affect non-canonical Wnt effectors (Jopling and Izpisua Belmonte, 2009; May-Simera and Kelley, 2012; Walentek et al., 2013). For example, Oteizas et al. have demonstrated that Wnt11 and Prickle-1a (*pck1a*) regulate planar cell polarity and KV (ergo, motile cilia) formation in zebrafish (Oteiza et al., 2010). To test the relationship between Nlz1 and non-canonical Wnt signaling pathway during ciliogenesis, expression of *wnt11* and *pck1a* was assayed by *in situ* hybridization in 1S stage embryos. *wnt11* is expressed in KV and DFCs, whereas *pck1a* was present in DFCs, but not KV (Figure 5A; data not shown). *nlz1* morphants show reduced or no expression of both of these genes in the DFCs and/or KV compared to control MO injected embryos (Fig. 5A,B; data not shown). Similarly, quantitative RT-PCR analysis revealed a 2.5 fold decrease in *wnt11* expression compared to control MO-injected embryos (Fig. 5C). Furthermore, Wnt11 mRNA was able to partially rescue the loss of motile cilia in KV (Fig. 5D–F) and the neuronal floor plate in approximately 50% of Nlz1 morphants (Fig. 5G–I). These data

suggest that *wnt11* is functionally downstream of *nlz1* and, consistent with published reports, that *wnt11* signaling contributes to cilia formation at KV.

Discussion

Nlz1 was originally described as a transcriptional co-repressor dynamically expressed during zebrafish development, particularly in the midbrain-hindbrain region (Runko and Sagerstrom, 2003). More recently, NLZ1 has been shown by several groups to be amplified in luminal breast cancers and to play an important role in regulating cell proliferation, migration, adhesion, and metastasis (Holland et al., 2011; Sircoulomb et al., 2011; Slorach et al., 2011). Here, we show that Nlz1 also plays an important and unexpected role in ciliogenesis in zebrafish KV, neural floorplate and pronephros via the transcription factor Foxj1a and both presumed canonical and non-canonical Wnt signaling. While many of the phenotypes observed in both the morphant and the mutant fish are reminiscent of ciliogenesis defects, *nlz1* also likely plays additional roles in development (e.g., regulation of Wnt signaling, discussed below).

Like *nlz1*, *foxj1a* is expressed in DFCs, KV, the neuronal floor plate, and the pronephros of zebrafish (Stubbs et al., 2008; Yu et al., 2008). Unlike *foxj1a*, overexpression of *nlz1* did not induce extra or ectopic cilia production; as such, Nlz1 function is likely necessary, but not sufficient for cilia formation in these structures. We posit that other proteins are also required for Foxj1a-mediated ciliogenesis. Also unlike the *foxj1a* morphants, knockdown of *nlz1* often resulted in hypoplasia of KV, consistent with its role in promoting cell division (Sircoulomb et al., 2011; Slorach et al., 2011). Although DFCs, as marked by *sox32* expression, were present in the KV of Nlz1 morphants, these cells did not go on to express the KV marker *cha*. This observation implies that *nlz1* may also be important in the cell specification program of KV cells.

Both canonical and non-canonical Wnt signaling have been implicated in ciliogenesis and cilia, in turn, may affect cell signaling through these and other pathways (Caron et al., 2012; He, 2008; May-Simera and Kelley, 2012). The relationship between Wnt signaling and cilia is, however, complex; published observations are sometimes contradictory (Wallingford and Mitchell, 2011), perhaps due to differences in experimental methods/models and even the definition of terms (e.g., “planar cell polarity” and “non-canonical Wnt”). It is this complexity that leads us to use terms such as “presumed canonical” and “presumed non-canonical” Wnt signaling in this study.

Wnt8a, a prototypical canonical Wnt (Hsieh et al., 1999) is required for KV specification and establishing left-right asymmetry (Lin and Xu, 2009); dorso-ventral patterning of the mesoderm; and antero-posterior neural patterning (Lekven et al., 2001). Caron et al. have recently shown that the beta-catenin serves as a direct regulator of the “master transcription factor” for motile ciliogenesis, *foxj1a* (Caron et al., 2012). Here, we extend these studies to show that during ciliogenesis in KV, the neural floor plate and the pronephros, *nlz1* is functionally downstream of both Wnt8a and Foxj1a signaling. While our *in vitro* data are consistent with direct binding of Foxj1a to *nlz1* upstream regulatory elements, the Foxj1a-independent effects of LiCl treatment on *nlz1* expression suggest that the epistatic

relationship between these molecules is likely more complex. The repression of beta-catenin signaling *in vitro* (Slorach et al., 2011) (this study) underscores this complexity and suggests a developmental feedback loop whereby Nlz1 negatively regulates canonical Wnt signaling.

Wnt11 is traditionally classified as an activator of non-canonical Wnt signaling (Uysal-Onganer and Kypta, 2012) and is required for convergent extension movements during zebrafish embryogenesis (Heisenberg et al., 2000). When higher doses (5ng) of Nlz1 morpholino were used in our experiments, we observed CE defects (data not shown), consistent with a role in non-canonical Wnt signaling. KV formation in zebrafish is, in part, regulated by Wnt11- and Pck1a- mediated changes to the specification and the cell adhesion properties of DFCs (Oteiza et al., 2010). The partial rescue of the KV phenotype in Nlz1 morphants suggests that Nlz1 acts upstream of Wnt11 in the process of KV formation and ciliogenesis. As such, Nlz1 appears poised in between presumed canonical Wnt (Wnt8a) and presumed non-canonical Wnt (Wnt11) signaling in the formation of KV and/or ciliogenesis.

Supplementary Material

Refer to Web version on PubMed Central for supplementary material.

Acknowledgments

We would like to thank Dr. Gaurav Varshney, Dr. Shawn Burgess, Dr. Albrecht Kramer-Zucker, and Dr. Igor Dawid for reagents and helpful discussion; Dr. Robert Fariss, and Dr. Chun Gao for technical support; Anna Larson, and Tyler Fayard for fish husbandry.

References

Ajima R, Hamada H. Wnt signalling escapes to cilia. Nature cell biology. 2011; 13:636–637. [PubMed: 21633348]

Amack JD, Yost HJ. The T box transcription factor no tail in ciliated cells controls zebrafish left-right asymmetry. Current biology : CB. 2004; 14:685–690. [PubMed: 15084283]

Babu D, Roy S. Left-right asymmetry: cilia stir up new surprises in the node. Open biology. 2013; 3:130052. [PubMed: 23720541]

Barrallo-Gimeno A, Holzschuh J, Driever W, Knapik EW. Neural crest survival and differentiation in zebrafish depends on mont blanc/tfap2a gene function. Development. 2004; 131:1463–1477. [PubMed: 14985255]

Brown JD, Dutta S, Bharti K, Bonner RF, Munson PJ, Dawid IB, Akhtar AL, Onojafe IF, Alur RP, Gross JM, Hejtmancik JF, Jiao X, Chan WY, Brooks BP. Expression profiling during ocular development identifies 2 Nlz genes with a critical role in optic fissure closure. Proceedings of the National Academy of Sciences of the United States of America. 2009; 106:1462–1467. [PubMed: 19171890]

Caron A, Xu X, Lin X. Wnt/beta-catenin signaling directly regulates Foxj1 expression and ciliogenesis in zebrafish Kupffer's vesicle. Development. 2012; 139:514–524. [PubMed: 22190638]

Chang L, Blain D, Bertuzzi S, Brooks BP. Uveal coloboma: clinical and basic science update. Current opinion in ophthalmology. 2006; 17:447–470. [PubMed: 16932062]

Corbit KC, Aanstad P, Singla V, Norman AR, Stainier DY, Reiter JF. Vertebrate Smoothened functions at the primary cilium. Nature. 2005; 437:1018–1021. [PubMed: 16136078]

Dorn KV, Hughes CE, Rohatgi R. A Smoothened-Evc2 Complex Transduces the Hedgehog Signal at Primary Cilia. Dev Cell. 2012

Essner JJ, Amack JD, Nyholm MK, Harris EB, Yost HJ. Kupffer's vesicle is a ciliated organ of asymmetry in the zebrafish embryo that initiates left-right development of the brain, heart and gut. Development. 2005; 132:1247–1260. [PubMed: 15716348]

Ferrante MI, Romio L, Castro S, Collins JE, Goulding DA, Stemple DL, Woolf AS, Wilson SW. Convergent extension movements and ciliary function are mediated by ofd1, a zebrafish orthologue of the human oral-facial-digital type 1 syndrome gene. Hum Mol Genet. 2009; 18:289–303. [PubMed: 18971206]

Fliegauf M, Benzing T, Omran H. When cilia go bad: cilia defects and ciliopathies. Nat Rev Mol Cell Biol. 2007; 8:880–893. [PubMed: 17955020]

Garcia-Gonzalo FR, Reiter JF. Scoring a backstage pass: mechanisms of ciliogenesis and ciliary access. J Cell Biol. 2012; 197:697–709. [PubMed: 22689651]

Gomperts BN, Gong-Cooper X, Hackett BP. Foxj1 regulates basal body anchoring to the cytoskeleton of ciliated pulmonary epithelial cells. J Cell Sci. 2004; 117:1329–1337. [PubMed: 14996907]

Grigoryan T, Wend P, Klaus A, Birchmeier W. Deciphering the function of canonical Wnt signals in development and disease: conditional loss- and gain-of-function mutations of beta-catenin in mice. Genes & development. 2008; 22:2308–2341. [PubMed: 18765787]

Hamada H, Meno C, Watanabe D, Saijoh Y. Establishment of vertebrate left-right asymmetry. Nature reviews Genetics. 2002; 3:103–113.

Hauptmann G, Gerster T. Two-color whole-mount in situ hybridization to vertebrate and Drosophila embryos. Trends in genetics : TIG. 1994; 10:266. [PubMed: 7940754]

He X. Cilia put a brake on Wnt signalling. Nature cell biology. 2008; 10:11–13. [PubMed: 18172427]

Heisenberg CP, Tada M, Rauch GJ, Saude L, Concha ML, Geisler R, Stemple DL, Smith JC, Wilson SW. Silberblick/Wnt11 mediates convergent extension movements during zebrafish gastrulation. Nature. 2000; 405:76–81. [PubMed: 10811221]

Hildebrandt F, Benzing T, Katsanis N. Ciliopathies. The New England journal of medicine. 2011; 364:1533–1543. [PubMed: 21506742]

Holland DG, Burleigh A, Git A, Goldgraben MA, Perez-Mancera PA, Chin SF, Hurtado A, Bruna A, Ali HR, Greenwood W, Dunning MJ, Samarajiwa S, Menon S, Rueda OM, Lynch AG, McKinney S, Ellis IO, Eaves CJ, Carroll JS, Curtis C, Aparicio S, Caldas C. ZNF703 is a common Luminal B breast cancer oncogene that differentially regulates luminal and basal progenitors in human mammary epithelium. EMBO molecular medicine. 2011; 3:167–180. [PubMed: 21337521]

Hsieh JC, Rattner A, Smallwood PM, Nathans J. Biochemical characterization of Wnt-frizzled interactions using a soluble, biologically active vertebrate Wnt protein. Proceedings of the National Academy of Sciences of the United States of America. 1999; 96:3546–3551. [PubMed: 10097073]

Huang T, You Y, Spoor MS, Richer EJ, Kudva VV, Paige RC, Seiler MP, Liebler JM, Zabner J, Plopper CG, Brody SL. Foxj1 is required for apical localization of ezrin in airway epithelial cells. J Cell Sci. 2003; 116:4935–4945. [PubMed: 14625387]

Jopling C, Izpisua Belmonte JC. Cilia--where two Wnts collide. Zebrafish. 2009; 6:15–19. [PubMed: 19250031]

Kimmel CB, Ballard WW, Kimmel SR, Ullmann B, Schilling TF. Stages of embryonic development of the zebrafish. Developmental dynamics : an official publication of the American Association of Anatomists. 1995; 203:253–310. [PubMed: 8589427]

Kishimoto N, Cao Y, Park A, Sun Z. Cystic kidney gene seahorse regulates cilia-mediated processes and Wnt pathways. Dev Cell. 2008; 14:954–961. [PubMed: 18539122]

Kramer-Zucker AG, Olale F, Haycraft CJ, Yoder BK, Schier AF, Drummond IA. Cilia-driven fluid flow in the zebrafish pronephros, brain and Kupffer's vesicle is required for normal organogenesis. Development. 2005; 132:1907–1921. [PubMed: 15790966]

Lan CC, Tang R, Un San Leong I, Love DR. Quantitative real-time RT-PCR (qRT-PCR) of zebrafish transcripts: optimization of RNA extraction, quality control considerations, and data analysis. Cold Spring Harbor protocols. 2009; 2009 pdb prot5314.

Lancaster MA, Schroth J, Gleeson JG. Subcellular spatial regulation of canonical Wnt signalling at the primary cilium. Nature cell biology. 2011; 13:700–707. [PubMed: 21602792]

Lekven AC, Thorpe CJ, Waxman JS, Moon RT. Zebrafish wnt8 encodes two wnt8 proteins on a bicistronic transcript and is required for mesoderm and neurectoderm patterning. Dev Cell. 2001; 1:103–114. [PubMed: 11703928]

Lewis JL, Bonner J, Modrell M, Ragland JW, Moon RT, Dorsky RI, Raible DW. Reiterated Wnt signaling during zebrafish neural crest development. Development. 2004; 131:1299–1308. [PubMed: 14973296]

Lim L, Zhou H, Costa RH. The winged helix transcription factor HFH-4 is expressed during choroid plexus epithelial development in the mouse embryo. Proceedings of the National Academy of Sciences of the United States of America. 1997; 94:3094–3099. [PubMed: 9096351]

Lin L, Spoor MS, Gerth AJ, Brody SL, Peng SL. Modulation of Th1 activation and inflammation by the NF-kappaB repressor Foxj1. Science. 2004; 303:1017–1020. [PubMed: 14963332]

Lin X, Xu X. Distinct functions of Wnt/beta-catenin signaling in KV development and cardiac asymmetry. Development. 2009; 136:207–217. [PubMed: 19103803]

May-Simera HL, Kelley MW. Cilia, Wnt signaling, and the cytoskeleton. Cilia. 2012; 1:7. [PubMed: 23351924]

McEwen DP, Jenkins PM, Martens JR. Olfactory cilia: our direct neuronal connection to the external world. Curr Top Dev Biol. 2008; 85:333–370. [PubMed: 19147011]

Neugebauer JM, Amack JD, Peterson AG, Bisgrove BW, Yost HJ. FGF signalling during embryo development regulates cilia length in diverse epithelia. Nature. 2009; 458:651–654. [PubMed: 19242413]

Nonaka S, Tanaka Y, Okada Y, Takeda S, Harada A, Kanai Y, Kido M, Hirokawa N. Randomization of left-right asymmetry due to loss of nodal cilia generating leftward flow of extraembryonic fluid in mice lacking KIF3B motor protein. Cell. 1998; 95:829–837. [PubMed: 9865700]

Norris DP, Grimes DT. Mouse models of ciliopathies: the state of the art. Disease models & mechanisms. 2012; 5:299–312. [PubMed: 22566558]

Oteiza P, Koppen M, Concha ML, Heisenberg CP. Origin and shaping of the laterality organ in zebrafish. Development. 2008; 135:2807–2813. [PubMed: 18635607]

Oteiza P, Koppen M, Krieg M, Pulgar E, Farias C, Melo C, Preibisch S, Muller D, Tada M, Hartel S, Heisenberg CP, Concha ML. Planar cell polarity signalling regulates cell adhesion properties in progenitors of the zebrafish laterality organ. Development. 2010; 137:3459–3468. [PubMed: 20843857]

Przemeck GK, Heinzmann U, Beckers J, Hrabe de Angelis M. Node and midline defects are associated with left-right development in Delta1 mutant embryos. Development. 2003; 130:3–13. [PubMed: 12441287]

Runko AP, Sagerstrom CG. Nlz belongs to a family of zinc-finger-containing repressors and controls segmental gene expression in the zebrafish hindbrain. Developmental biology. 2003; 262:254–267. [PubMed: 14550789]

Sircoulomb F, Nicolas N, Ferrari A, Finetti P, Bekhouche I, Rousselet E, Lonigro A, Adelaide J, Baudelet E, Esteyries S, Wicinski J, Audebert S, Charafe-Jauffret E, Jacquemier J, Lopez M, Borg JP, Sotiriou C, Popovici C, Bertucci F, Birnbaum D, Chaffanet M, Ginestier C. ZNF703 gene amplification at 8p12 specifies luminal B breast cancer. EMBO molecular medicine. 2011; 3:153–166. [PubMed: 21328542]

Slorach EM, Chou J, Werb Z. Zeppo1 is a novel metastasis promoter that represses E-cadherin expression and regulates p120-catenin isoform expression and localization. Genes & development. 2011; 25:471–484. [PubMed: 21317240]

Stubbs JL, Oishi I, Izpisua Belmonte JC, Kintner C. The forkhead protein Foxj1 specifies node-like cilia in Xenopus and zebrafish embryos. Nature genetics. 2008; 40:1454–1460. [PubMed: 19011629]

Supp DM, Witte DP, Potter SS, Brueckner M. Mutation of an axonemal dynein affects left-right asymmetry in inversus viscerum mice. Nature. 1997; 389:963–966. [PubMed: 9353118]

Thisse C, Thisse B. High-resolution in situ hybridization to whole-mount zebrafish embryos. Nature protocols. 2008; 3:59–69. [PubMed: 18193022]

Uysal-Onganer P, Kypta RM. Wnt11 in 2011 - the regulation and function of a non-canonical Wnt. Acta physiologica. 2012; 204:52–64. [PubMed: 21447091]

Walentek P, Schneider I, Schweickert A, Blum M. Wnt11b is involved in cilia-mediated symmetry breakage during Xenopus left-right development. PloS one. 2013; 8:e73646. [PubMed: 24058481]

Wallingford JB, Mitchell B. Strange as it may seem: the many links between Wnt signaling, planar cell polarity, and cilia. Genes & development. 2011; 25:201–213. [PubMed: 21289065]

Westerfield, M. The zebrafish book; A Guide for the Laboratory Use of zebrafish (*Danio rerio*). University of Oregon Press; Eugene, OR: 2000.

Yu X, Ng CP, Habacher H, Roy S. Foxj1 transcription factors are master regulators of the motile ciliogenic program. Nature genetics. 2008; 40:1445–1453. [PubMed: 19011630]

Zaghloul NA, Brugmann SA. The emerging face of primary cilia. Genesis. 2011; 49:231–246. [PubMed: 21305689]

Highlights

- Nlz1 is necessary for motile cilia formation.
- Canonical Wnt signaling induces *nlz1* expression.
- FoxJ1a acts upstream of Nlz1.
- Wnt11 is functionally downstream of Nlz1.

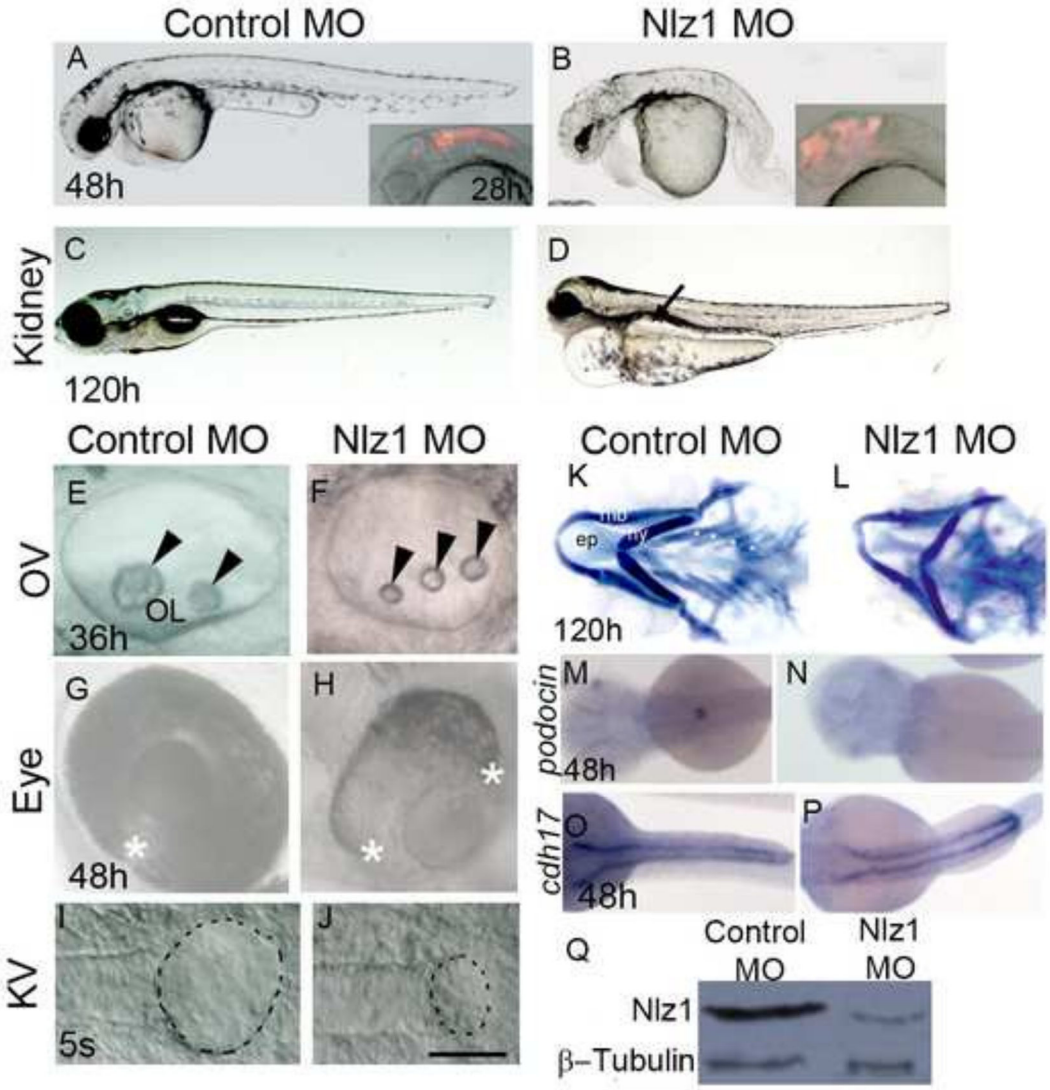

Fig 1. Nlz1 morpholino-injected embryos show morphological defects similar to a human ciliopathy

(A–J) DIC images of live embryos at different developmental stages (A,B,G,H) 48h; (C,D) 120h; (E,F) 36h; (I,J) 5S. Embryos were injected with Control MO (A,C,E,G,I) or with Nlz1 MO (B,D,F,H,J) at the 1–2 cell stage. Nlz1 MO injected embryos show generalized edema; an abnormal brain; a short, bent tail (B); kidney cyst(s) (D, arrow, n=45/55); three small otoliths in the OV (F, arrow head, n=52/60); and a rudimentary KV (J, dotted line, n=15/40). In control MO injected embryos, gross morphology (A), kidneys (C), otoliths (E), and KV (I) were normal. Control MO injected embryos (A, inset), and *nlz1* morphants (B, inset) were injected with rhodamine dextran in the hindbrain ventricles at 28h. The two edges of the optic fissure were fused completely in control MO injected embryos (G, asterisk, n= 50/50) whereas coloboma was observed in *nlz1* morphants (H, n=72/80). (K–L) Alcian blue staining of pharyngeal cartilages in control MO (K) and Nlz1 MO (L) injected zebrafish larvae at 120h. (M–P) Dorsal view of a whole mount *in situ* hybridization with probes for

podocin (M,N), and *cdh17* (O,P) in control MO (M,O) and Nlz1 MO (N,P) injected embryos at 48h. (Q)Western blot shows severe reduction of Nlz1 protein expression in morphants. (B,F,H,J) injected with 3.5ng Nlz1 MO, (D,L,N,P) injected with 2ng Nlz1 MO. (A–H) lateral views, anterior to the left; (I–J) dorsal view, posterior to the top. Scale bar in A–B, and insets, 320μm; C–D, 200μm; E–F, 35μm; G–H, 100μm; I–J, 50μm. OV, otic vesicle; KV, Kupffer's vesicle; OL, otolith; s, somite; ep, ethmoid plate; mb, mandibular arch; hy, hyoid arch; asterisks indicate branchial arches.

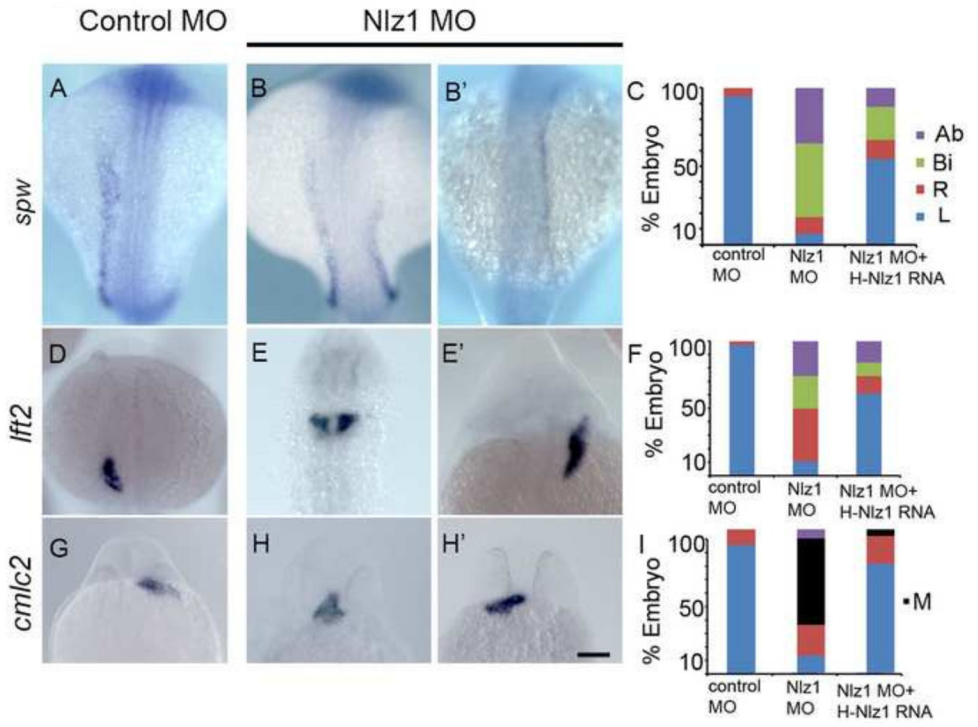

Fig 2. Nlz1 is important for left-right patterning in zebrafish

Zebrafish embryos were injected with control MO (A,D,G) or with 2 ng of Nlz1 MO (B,B′,E,E′,H, H′). Embryos were hybridized *in situ* with laterality marker genes *spw* (A,B,B′), *lft2* (D,E,E′), and *cmlc2* (G,H,H′) RNA probes. Quantification of expression patterns of *spw* (C), *lft2* (F), and *cmlc2* (I) in MO (*spw*, n=85; *lft2*,n=110; *cmlc2*, n=75) and MO + mRNA injected embryos (*spw*, n=75; *lft2*,n=100; *cmlc2*, n=55). (A,B,B′,D,E,E′) dorsal view at 18–20S stage, (G,H,H′) frontal view at 28 h. Scale bar 100μm. Ab: absent; Bi: bilateral, M: midline; R: right; L: left.

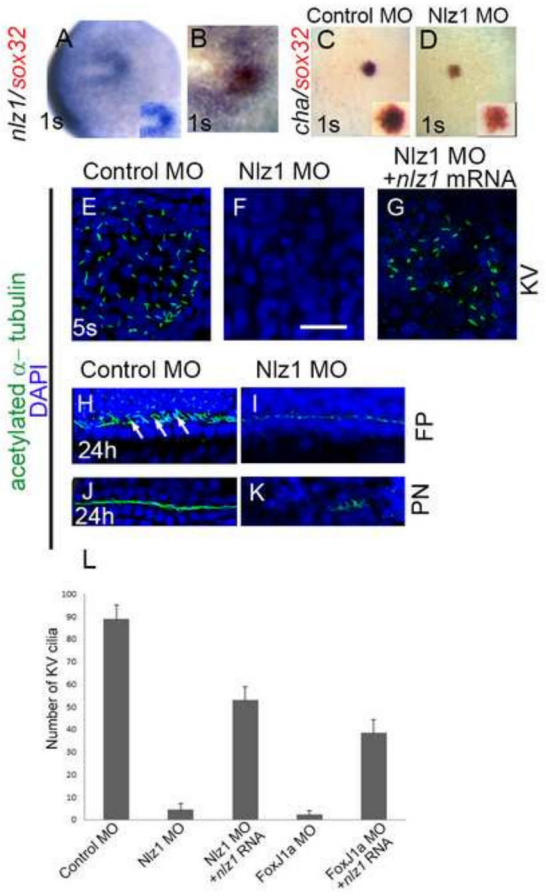

Fig 3. *nlz1* is expressed in Kupffer's vesicle and is required for cilia formation in zebrafish

Whole mount *in situ* hybridization at the one somite (1S) stage with one or two RNA probes as indicated in wild type (A, B), control MO injected (C), and Nlz1 MO injected (D) embryos. (B) Cells in the KV co-express *nlz1* and *sox32*, marking dorsal forerunner cells. In *nlz1* morphants *cha* (D, n=28/35) was absent in the KV region, whereas *sox32* (red) remained unaltered as compared to control MO injected embryos(C). Cilia were marked with acetylated-α tubulin (green) and nuclei were counterstained with DAPI (blue) in different region of the embryos as indicated. Complete absence of KV cilia was observed in *nlz1* morphants (F, n=15/18) compared to control (E, n=15/15). Similarly, at later stages, the number and length of the cilia in the neural FP (I, n=18/23) and in the PN (K, n=27/30) were reduced in *nlz1* morphants compared to control MO injected embryos (H, J,). Arrows indicate motile cilia. KV cilia in *nlz1* morphants were rescued by *nlz1* mRNA injection (G, n=45/52). (L) Quantification of cilia number in KV embryos injected with MO ± mRNA. (A, B) dorsal view, anterior to left; (C–D) dorsal view, posterior to top. (D,F,G) injected with 2.5ng Nlz1 MO, (I,K) injected with 2ng Nlz1 MO. Inset (A, C, D) shows blow up of KV region. KV; Kupffer's vesicle; s, somite; FP, floor-plate; PN, pronephros. Scale bar in A–D, 100μm;E–G, 12.5μm; H–K, 50μm.

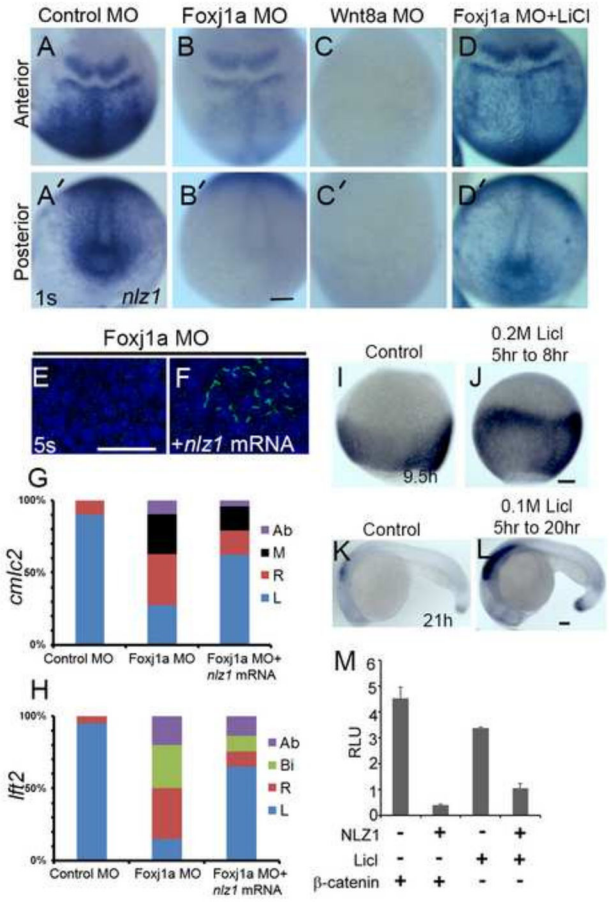

Fig 4. Nlz1 is downstream of Foxj1a and is regulated by canonical Wnt signaling

(A–D, A′–D′) *nlz1* expression in *foxj1a* morphants (B, B′, n=48/50), *wnt8a* morphants (C,C′, n=52/55), and LiCl treated *foxj1*morphants embryos (D,D′, n=25/28) compared to control MO (A,A′, n=30/30), as seen in whole mount *in situ* hybridization of embryos at 1S stage. (E–F) Cilia are labeled with anti-acetylated α tubulin antibody (green) in the KV at the 5S stage. Complete lack of KV cilia was observed in *foxj1a* morphants (E, n=20/20); injection of *nlz1* mRNA in *foxj1a* morphants rescues KV cilia (F, n=12/30). Quantification of expression patterns of *cmlc2* (G), and *lft2* (H) in Foxj1a MO (*cmlc2*, n=50; *lft2*,n=50) and Foxj1a MO + *nlz1*mRNA (*cmlc2*, n=50; *lft2*,n=50) injected embryos. (A–F) dorsal view, (A–D) anterior dorsal, (A′–D′) posterior dorsal, (E, F) posterior to the top. (H,J) Embryos were treated with LiCl as specified. (I–L) Whole mount *in situ* hybridization at 95% epiboly (I, J) and 21h (K, L) resulted in expansion of *nlz1* expression (J, n=45/50; L, n=15/19) compared to control (I n=40,K n=40, without LiCl). (I, J) dorsal view, (K,L) lateral view, anterior to left. (M) Nlz1 repressed Wnt/β-catenin signaling activated by either LiCl or β-catenin in a TOPflash luciferase assay. RLU, relative luciferase units. Ab: absent; Bi: bilateral, M: midline; R: right; L: left. Scale bar (black) in A–D′, 100μm; I–J, 60μm; K–L, 75μm. Scale bar (white) in E–F, 50μm.

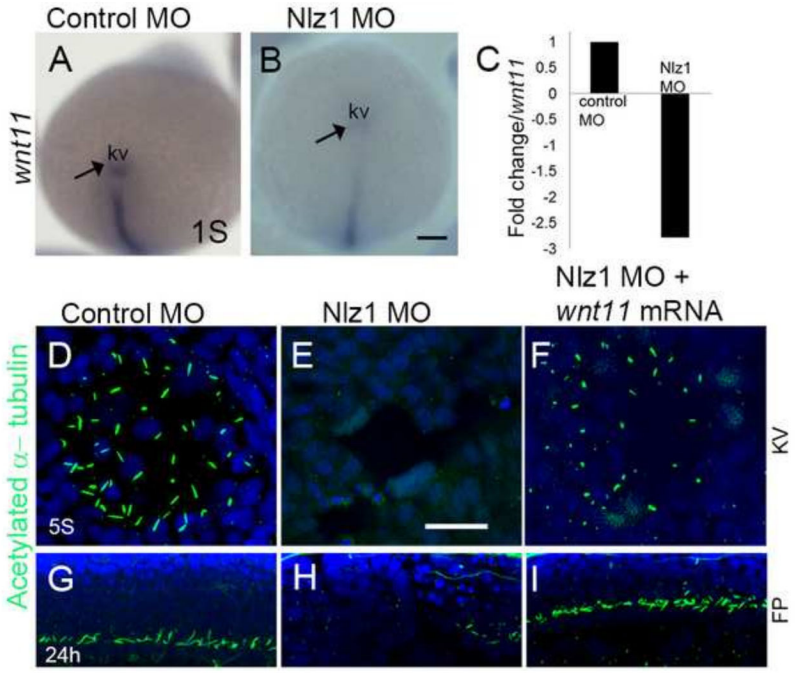

Fig 5. *wnt11* rescues cilia defects in *nlz1* morphant fish

(A,B) Whole mount *in situ* hybridization at 3S stage with *wnt11* antisense RNA probe as indicated in (A) control MO injected, and (B) Nlz1 MO injected embryos. (C) Bar diagram demonstrating down-regulation of *wnt11* expression (~2.5 fold) in *nlz1* morphant embryos compare to control. (D–F) Cilia were labeled with anti-acetylated tubulin in KV, and (G–I) in FP. Motile cilia were absent in KV and FP of *nlz1* morphants (E n=28/32, H n=17/24), compared to control MO injected embryos (D n=40/40, G n=40/40). Co-injection of wnt11 mRNA and Nlz1 MO (F n=20/41, I n=25/41) partially rescues cilia in KV and the FP. (A, B) posterior view. KV; Kupffer's vesicle; s, somite; FP, floor-plate. Scale bar A and B, 100μm; D–F, 12.5μm; G–I, 50μm.